

Sub-GeV $U(1)_R$ gauge boson to address the proton radius discrepancy

Carlos Alvarado,^{1,*} Alfredo Aranda,^{2,1,†} and Cesar Bonilla^{3,1,‡}

¹*Dual CP Institute of High Energy Physics, C.P. 28045, Colima, México*

²*Facultad de Ciencias, Universidad de Colima, Colima 28010, Mexico.*

³*Departamento de Física, Universidad Católica del Norte,
Avenida Angamos 0610, Casilla 1280, Antofagasta, Chile.*

We propose a Standard Model extension by a $U(1)_R$ gauge symmetry where only right-handed chiral fermions can carry a non-trivial charge. Here we show that the simplest anomaly-free solution to accommodate the proton charge radius discrepancy takes right-handed muons μ_R and first generation quarks, u_R and d_R . Consistency with the latest muon's $(g-2)$ measurements is achieved through an extra light scalar, which itself must lie in the tens of MeV mass range to be viable.

I. INTRODUCTION

The Standard Model (SM) of particle physics successfully describes three of the four known fundamental interactions of nature: electromagnetic, weak, and strong. The tremendous accuracy of the SM has been corroborated by contemporary collider experiments at high energies such as the Large Hadron Collider (LHC). Nevertheless, this and other experiments have found several subtle deviations from the SM predictions that remain to be accounted for. For some of these anomalies, if they persist and get confirmed, the presence of new physics is required.

Some of those deviations have received particular attention during the last decade with revitalized interest provided by new measurements. It is peculiar that they all somehow involve the muon, suggesting that subtle effects in its interactions might be a key to new physics. Examples are the B -meson anomalies, which are deviations from the SM predictions in angular observables and the ratios $R_{K(K^*)} = \mathcal{B}r(B \rightarrow K^{(*)}\mu^-\mu^+)/\mathcal{B}r(B \rightarrow K^{(*)}e^-e^+)$ that might point to violation of lepton-flavor universality. These have captured a lot of theoretical interest with plenty of effort channeled towards setups that extend the SM with additional scalars and/or gauge bosons coupled to quarks and leptons in a non-universal manner [1]. As of today, the deviations persist at a level above 3σ , based on the latest results from the LHCb collaboration at the LHC [2, 3]. Another example of anomalies is the latest measurements of the muon's $(g-2)$ [4], for which attempts to accommodate it within SM extensions containing *muonic* mediators already comprises a vast literature.

Our focus is in yet another instance of tentative new physics involving the muon. For decades, the study of the structure of the hadrons found in nuclei —protons and neutrons—has improved as a result of increasingly refined techniques such as lepton-nucleon scattering and the spectroscopy of hydrogen-like atoms. Among the long-standing studied observables there is the (root-mean-square) proton charge radius, r_p . Despite the good agreement between measurements of r_p by experiments involving electrons prior to 2010, in that year the CREMA collaboration found a highly discrepant r_p value through spectroscopy of hydrogen-like atoms where the muon replaces the electron (muonic hydrogen) [5]. The muonic result improved in 2013 [6] and continued to be discrepant with the electronic-measurement

* calvara@dcphep.com

† fefo@ucl.mx

‡ cesar.bonilla@ucn.cl

averages compiled and published by the CODATA committee in 2014 [7]

$$\begin{aligned} r_p^{(e)} &= 0.8751 \pm 0.0061 \text{ fm} \\ r_p^{(\mu)} &= 0.84087 \pm 0.00039 \text{ fm} . \end{aligned} \tag{1}$$

Fast forward to 2021, several experiments with electrons and form-factor analyses of the data have found a degree of consistency with the muonic r_p value. In particular the CODATA 2018 average [8] and posterior reports [9] tend to favor the muonic r_p value. Yet, since a few other recent experimental collaborations [10, 11] have reported r_p values that persistently agree with the CODATA 2014 r_p value, the proton charge radius puzzle is certainly ameliorated but not conclusively gone¹ [10, 11]. Similarly, given that the value found by Grinin et. al. [14] is offset the muonic value by about two standard deviations, the puzzle is kept alive.

With the ongoing progress in higher order theoretical corrections in scattering and spectroscopy and the projected sensitivity of near-future experiments, the community has also entertained the possibility that these r_p discrepancies are a hint of new physics consisting on muonphilic interactions of the proton [15–18]. This is the approach taken in this paper: we follow the hypothesis that the Δr_p^2 discrepancy between the two values in Eq. (1) will persist, and is addressed by new degrees of freedom of a complete, anomaly-free gauge $U(1)$ model. Our setup is also consistent with other relevant constraints, including LHC bounds on new scalars and those from the latest muon ($g-2$) results by Fermilab [4, 19] and the Lattice QCD group [20].

Our work is organized as follows: the new gauge model and its field content is described in in Sec. II, with the proton charge radius discrepancy reviewed and addressed in Sec. III. Contributions to the muon’s ($g-2$) are discussed in Sec. IV, where we also study numerically the parameter space where r_p can be accomodated while consistent with collider limits on scalars and the muon’s ($g-2$). Closing remarks follow afterwards.

II. MODEL SELECTION

In this scenario the SM gauge group is enlarged by an Abelian gauge $U(1)_R$ symmetry (and its corresponding Z' gauge boson) where only right-handed(RH) chiral fermions may have non-trivial transformation under the new symmetry. Specifically, only first generation RH quarks and the RH muon are charged under the new $U(1)_R$ gauge symmetry².

In addition, the model contains the following $U(1)_R$ -charged scalars, needed to break $U(1)_R$ spontaneously and give a mass to the Z' : a complex SM singlet s , and a $SU(2)_L$ doublet Φ_2 (same hypercharge as the SM Higgs field, denoted as Φ_1) which will also be responsible for generating the masses of the muon, up, and down quarks. As it is shown in the next section, due to its relative size to the vacuum expectation value (vev) of Φ_2 , the vev of s generates most of the Z' mass while accomodating the charge radius discrepancy. Meanwhile, a range of sizes for the Φ_2 vev is discussed at the end of this section. The rest of the SM particles are uncharged under the new symmetry, including the Higgs-like doublet.

The fact that SM fermions of different generations carry distinct $U(1)_R$ quantum numbers implies that gauge anomalies do not cancel automatically per generation, thus extra (chiral) fermion content is needed to satisfy the anomaly-free conditions. For this purpose one SM singlet RH neutrino ν_R is introduced into the model (with a yet unspecified charge $q_\nu \neq 0$ that does the job when exactly one quark and one lepton generations are charged³).

¹ Two comprehensive reviews on the proton charge radius are found in Refs. [12] and [13].

² Other examples and uses of Abelian gauge extensions can be found in Refs. [21, 22].

³ ν_R is not tied to the any lepton generation.

Given the introduction of the SM singlet ν_R , there are 27 different anomaly-free scenarios that one could generate. The diagram in Fig. 1 exemplifies the 9 gauge anomaly-free combinations involving the RH u -quark, with all three RH d -type quarks and RH charged leptons. The other 18 solutions involve c_R and t_R . Seeking to establish a connection between nucleons and muons that tackles the proton radius puzzle, the valence RH-quarks of the first generation and the second generation lepton are the ones given a non-trivial charge under $U(1)_R$. This choice is illustrated by the solid red line in Fig. 1. For reference, Table I displays the rest of anomaly-free charge assignments of the model's matter content in terms of an arbitrary charge q_ν .

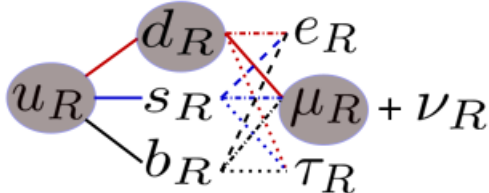


FIG. 1: Set of right-handed fermion combinations free of gauge anomalies. The solid red line connecting the three blobs illustrates the link between nucleons and muons as demanded by the proton radius puzzle.

	$Q_{L(1,2,3)}$	u_R	(c_R, t_R)	d_R	(s_R, b_R)	$L_{(1,2,3)}$	(e_R, τ_R)	μ_R	ν_R	Φ_1	Φ_2	s
$SU(2)_L$	2	1	1	1	1	2	1	1	1	2	2	1
$U(1)_R$	0	q_ν	0	$-q_\nu$	0	0	0	$-q_\nu$	q_ν	0	q_ν	q_s

TABLE I: Particles with nonzero gauge $U(1)_R$ charge assignments.

We choose to work out the $q_\nu = +1$ solution for the sake of generality. In this scenario, a Dirac neutrino mass is generated through the Yukawa term $\sim \bar{L}_L \nu_R \tilde{\Phi}_2$, whose smallness might be associated to the small induced vev of the additional $SU(2)$ scalar doublet as in the type-II seesaw for Dirac neutrinos [23]. In order to account for all neutrino oscillation observables the model can be further extended with extra RHNs neutral or not under $U(1)_R$. The actual construction of the neutrino sector is out of the scope of this paper.

A. New interactions

The relevant operators and scalar potential are listed next. The fermion interactions with the Z' are given by

$$\mathcal{L}_{\text{gauge}} \supset (g' q_\nu) Z'^\mu [\bar{u}_R \gamma_\mu u_R - \bar{d}_R \gamma_\mu d_R - \bar{\mu}_R \gamma_\mu \mu_R + \bar{\nu}_R \gamma_\mu \nu_R] . \quad (2)$$

Then, the overall right- and left-handed couplings $C_{R,L}$ to the muon become $C_R = -g'$ and $C_L = 0$ for $q_\nu = 1$. We normalize the vector (V) and axial vector (A) couplings as $C_{V,A} = \frac{1}{2}(\pm C_L + C_R)$. The gauge-invariant Yukawas of the SM fermions are

$$\begin{aligned} -\mathcal{L}_Y &= y_{ie} \bar{L}_i e_R \Phi_1 + y_{i\mu} \bar{L}_i \mu_R \Phi_2 + y_{i\tau} \bar{L}_i \tau_R \Phi_1 + y_{i\nu} \bar{L}_i \nu_R \tilde{\Phi}_2 \\ &+ y_{id} \bar{Q}_i d_R \Phi_2 + y_{is} \bar{Q}_i s_R \Phi_1 + y_{ib} \bar{Q}_i b_R \Phi_1 \\ &+ y_{iu} \bar{Q}_i u_R \tilde{\Phi}_2 + y_{ic} \bar{Q}_i c_R \tilde{\Phi}_1 + y_{it} \bar{Q}_i t_R \tilde{\Phi}_1 + \text{H.c.} \end{aligned} \quad (3)$$

with $i = 1, 2, 3$ denoting the fermion generations and where

$$\Phi_a = \begin{pmatrix} \varphi_a^+ \\ \varphi_a^0 \end{pmatrix} = \begin{pmatrix} \varphi_a^+ \\ \frac{v_{\Phi_a} + \varphi_{aR}^0 + i\varphi_{aI}^0}{\sqrt{2}} \end{pmatrix}, \quad \text{with } a = 1, 2. \quad (4)$$

Regarding the generation of the muon mass, we consider the Yukawa matrix for charged lepton as diagonal, so that, $y_{2\mu} \neq 0$. Thus from (3) $m_\mu = y_{2\mu} v_{\Phi_2} / \sqrt{2}$. A *natural* muon Yukawa occurs if one selects $v_{\Phi_2} \approx m_\mu$ within one order of magnitude. Then $0.01 \lesssim v_{\Phi_2} / \text{GeV} \lesssim 1$ is equivalent to $0.1 \lesssim y_{2\mu} \lesssim 10$, with the possibility of saturating $y_{2\mu} = 4\pi$. The sizability of v_{Φ_2} (or equivalently $y_{2\mu}$) will prove to be important in Sec. IV to accomodate the $(g-2)_\mu$ bounds. The scalar potential of our Two-Higgs doublet model (2HDM) plus complex singlet reads

$$\begin{aligned} V(\Phi_1, \Phi_2, s)_{q_s=-1/2} = & -\mu_1^2 \Phi_1^\dagger \Phi_1 - \mu_2^2 \Phi_2^\dagger \Phi_2 - \mu_s^2 s^* s + \lambda_1 (\Phi_1^\dagger \Phi_1)^2 + \lambda_2 (\Phi_2^\dagger \Phi_2)^2 + \lambda_s (s^* s)^2 \\ & + \lambda_{12} \Phi_1^\dagger \Phi_1 \Phi_2^\dagger \Phi_2 + \lambda'_{12} \Phi_1^\dagger \Phi_2 \Phi_2^\dagger \Phi_1 + \lambda_{1s} \Phi_1^\dagger \Phi_1 s^* s + \lambda_{2s} \Phi_2^\dagger \Phi_2 s^* s + \kappa (s^2 \Phi_1^\dagger \Phi_2 + \text{h.c.}), \end{aligned} \quad (5)$$

where the $U(1)_R$ charge of the scalar singlet is taken as $q_s = -1/2$. For this charge choice, the allowed four-scalar operator with the Higgs doublets is $s^2 \Phi_1^\dagger \Phi_2$, with dimensionless coefficient κ as in Ref. [23]. An alternative, not pursued here, is choosing $q_s = -1$ under which the allowed four-scalar operator would be $s \Phi_1^\dagger \Phi_2$ with a dimensionful mass parameter as coefficient.

III. THE CHARGE RADIUS DISCREPANCY

In our model the contributions to the proton charge radius come from the exchange of the mediators Z' , Φ_2 and s between muons and protons. We later discuss why the scalar contributions are subleading/negligible. Furthermore, since left-handed chiral neutrinos do not interact with the nucleus through the Z' , they automatically avoid neutrino-nucleon scattering constraints [16].

The energy splitting in muonic hydrogen by exchange of the vectorial (V) component of a spin-1 mediator is given by [15]

$$|\Delta E^{(V)}| = \frac{|C_V^\mu C_V^p|}{4\pi} \frac{m_V^2 (m_{\text{red}} \alpha_{\text{em}})^3}{2(m_V + m_{\text{red}} \alpha_{\text{em}})^4}, \quad (6)$$

with the analog $\Delta E^{(S)}$ by CP-even scalar exchange⁴ sharing the same expression. Above, the $C_V^{\mu(p)}$ are the vectorial muon (proton) couplings to the gauge boson, $m_{\text{red}} \equiv m_p m_\mu / (m_\mu + m_p)$ is the muon-proton reduced mass, m_V is the mediator mass, and α_{em} is the QED constant. The Lamb energy shift between levels $2S_{1/2}$ and $2P_{1/2}$ depends on the radius r (in fm) through the following relation [12],

$$\Delta E(r) = 206.0336 - 5.2275r^2 + 0.0332\text{MeV}. \quad (7)$$

So we are using Eq. (7) to fit the proton charge radius discrepancy shown in Eq. (1). This will correspond to an energy shift of $\Delta E \approx 306.4 \mu\text{eV}$.

For purposes of simplicity, we take the Z' coupling to the u and d quarks as an estimate of C_V^p , the vectorial Z' coupling to the proton⁵. Then from Eq. (2), with $C_V^\mu = C_V^p \equiv C_V[Z']$, the relevant Z' coupling appearing in the energy shift (6) is $|C_V[Z']| = g'/2$. In addition, in (6) $m_V = m_{Z'}$, which in our setup is $m_{Z'} \approx g' \sqrt{(v_s^2/4) + v_{\Phi_2}^2}$.

⁴ Pseudoscalar contributions are tiny according to [15].

⁵ The proportionality factor between quark- Z' couplings and proton- Z' couplings is determined through the sum of the constituent quark charges (vectorial) and through matrix elements techniques (axial).

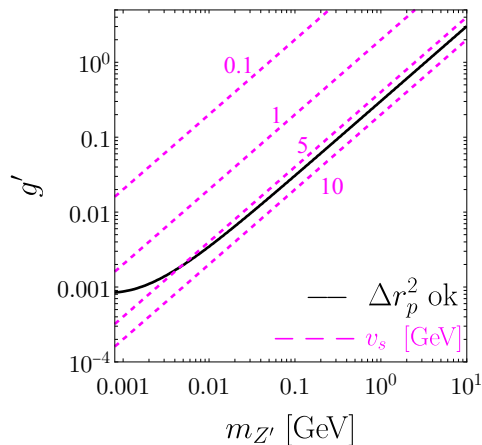


FIG. 2: Z' mass-coupling curve fitting the Δr_p^2 discrepancy (solid black) obtained from equating the RHS of Eq. (6) to $306.4 \mu\text{eV}$, and the corresponding $U(1)_R$ -breaking singlet vev (magenta dashed).

The square of this value is the diagonal entry of the new gauge boson in the full 3×3 interaction-basis mass matrix of the neutral vector bosons after the Weinberg rotation. In the limit of vanishing kinetic mixing, this value is a good approximation for $m_{Z'}$ because the off-diagonal mass mixing of the $U(1)_Y$ and $U(1)_R$ gauge bosons goes as $-\frac{1}{2}g'\sqrt{g_1^2 + g_2^2}v_{\Phi_2}^2$ and this is much smaller than $|m_{Z'}^2 - m_Z^2|$ (see for example the parametrization of Ref. [24]).

On the $(m_{Z'}, g')$ plane in Fig. 2, a solid black curve satisfying $|\Delta E^{(V)}| \approx 306.4 \mu\text{eV}$ is shown, together with a few contours of the corresponding v_s singlet vev (magenta dashed), which we will assume dominates the Z' mass, i.e. $m_{Z'} \approx g'v_s/2$. These dashed contours indicate that $5 \lesssim v_s/\text{GeV} \lesssim 10$ works well for Δr_p^2 , except when $m_{Z'}$ gets as low as 1 MeV⁶.

With the previous information it is suggested that the proton radius puzzle can be addressed in this model thanks *only* to existence of a light Z' that interacts only with one family of RH-quarks and -leptons. However, the assumption on the vevs ($v_s \sim \text{few GeVs} \gg v_{\Phi_2} \sim m_\mu$) has an impact on the scalar mass spectrum which is constrained by current experimental data. Moreover, given the features of the model, we will also consider the latest muon ($g-2$) results, which provide important parameter space restrictions and predictions.

IV. MODEL CONSTRAINTS AND RESULTS

In what follows we will describe the experimental limits applied to our setup. As discussed earlier, from Fig. 2, and under our choice $q_s = -1/2$, a vev $v_s \approx 6.5 \text{ GeV}$ fits Δr_p^2 for $m_{Z'}$ above 1 MeV. This and other parameters choices will be collected in Table II, where subindices will be dropped for the muon Yukawa, $y \equiv y_{2\mu}$, to ease notation. Now we proceed to discuss the scalar sector and its experimental restrictions.

A. Limits on the scalar mass spectrum

The singly-charged Higgs from the Φ_2 doublet is subject to severe LHC constraints. In the context of a muonphilic 2HDM, a bound $m_{H^+} \gtrsim 640 \text{ GeV}$ has been reported [25]. We choose two representative benchmarks, one with the

⁶ This curve's behavior is due to the constant term in denominator of Eq. (6).

m_{H_3}, m_A, m_{H^+} sitting right at this bound, and another, more conservative one where they sit at 1 TeV. In order to have a grip on the s -like and φ_2 -like scalar masses, we look closer at the mass matrices in a regime of small mixing. For a $O(1)$, sizable κ coupling and under the vev hierarchy $v_{\Phi_1} \gg v_s \gg v_{\Phi_2}$, the M_R^2 mixing matrix in (A3) can always be brought to an approximate block-diagonal form

$$M_R^2 \sim \begin{pmatrix} 2\lambda_1 v_{\Phi_1}^2 & \varepsilon & \varepsilon' \\ \varepsilon & 2\lambda_s v_s^2 & -\kappa v_{\Phi_1} v_s \\ \varepsilon' & -\kappa v_{\Phi_1} v_s & \kappa v_{\Phi_1} v_s^2 / (2v_{\Phi_2}) \end{pmatrix} \quad (8)$$

under a suitable choice of quartics. Above, $\varepsilon, \varepsilon'$ entries are no larger than the (1, 1) entry, but much smaller than the (3, 3) and (2, 3) entries. Then the diagonalization of the lower-right 2×2 block in $(\sigma_R, \varphi_{2R}^0)$ approximates the light s -like and φ_2 -like masses, and it does it in terms of $\lambda_s, \kappa, v_{\Phi_2}$ only (recall that $v_{\Phi_1}^2 = (246 \text{ GeV})^2 - v_{\Phi_2}^2$, and that v_s is fixed by Δr_p^2). The approximate eigenvalues of this block are

$$m_{\text{light,heavy}}^2 = \frac{1}{2} (2\lambda_s v_s^2 + \kappa v_{\Phi_1} v_s^2 / (2v_{\Phi_2})) \mp \sqrt{\frac{1}{4} [2\lambda_s v_s^2 - \kappa v_{\Phi_1} v_s^2 / (2v_{\Phi_2})]^2 + (-\kappa v_{\Phi_1} v_s)^2} . \quad (9)$$

At next-to-leading order in v_{Φ_2} , the light mass is

$$m_{\text{light}} \approx \sqrt{2(\lambda_s v_s^2 - \kappa v_{\Phi_1} v_{\Phi_2})} , \quad (10)$$

whereas the heavy one is well approximated by the diagonal entry in φ_{2R} at leading order in v_{Φ_2}

$$m_{\text{heavy}} \approx \sqrt{\frac{\kappa}{2} \frac{v_{\Phi_1}}{v_{\Phi_2}} v_s} . \quad (11)$$

The charged scalar mass is also approximated by (11), and this is also true for the pseudoscalar A too. Therefore, the H_3, A, H^+ in this regime are highly degenerate. Given these masses, m_{heavy} is freed from the 640 GeV bound by LHC on charged scalars if

$$\sqrt{\kappa/v_{\Phi_2}} \gtrsim 8.88 \text{ GeV} . \quad (12)$$

Regarding the s -like singlet scalar, its mass m_{light} must be rather light in order to help the total Δa_μ reach the current limit. Since its coupling to muons is suppressed by the small s - Φ_2 mixing, y must be large enough to compensate. At light mass values, however, a tachyonic m_{light} must be avoided. This is achieved if

$$|\lambda_s v_s^2 - \kappa v_{\Phi_1} v_{\Phi_2}| \geq 0 . \quad (13)$$

Contours of the light singlet (solid green) and charged scalar (dashed orange) masses are shown in the panels of Fig. 3 in the (κ, λ_s) plane, at two representative, fixed Yukawa values (i.e. fixed v_{Φ_2}), $y=1$ and $y=4\pi$. A tachyonic m_{light} for the singlet is developed over the gray region. A noticeable feature is that the new doublet vev must be sufficiently smaller than $v_{\Phi_2} \sim 0.1 \text{ GeV}$ for the singlet mass contours to be freed from the LHC limit on muonphilic H^+ , which pushes y to values larger than 1. For reference, the conservative LEP constraint on H^+ is shown as well.

Two zooms of the right panel of Fig. 3 are displayed in Fig. 4. The dashed green contours in the panels are m_{light} values from the full 3×3 mixing matrix. The deviation with respect to the contours of the 2×2 subblock (solid green) is small as long as the approximate form (8) holds. One observes that regions with (non-tachyonic) sub-GeV m_{light} and $m_{\text{heavy}} \gtrsim 640 \text{ GeV}$ are narrow and very sensitive to κ, λ_s . The model is then said to demand a singlet-like scalar in a well-defined range of tens of MeV.

We list the mass spectrum at two benchmarks in Table II, and mark them with red crosses in the panels of Fig. 3. Notice that the charge scalar mass m_{H^+} sits at either 640 GeV or 1 TeV, with $m_A \approx m_{H^+} \approx m_{H_3}$ in both benchmarks.

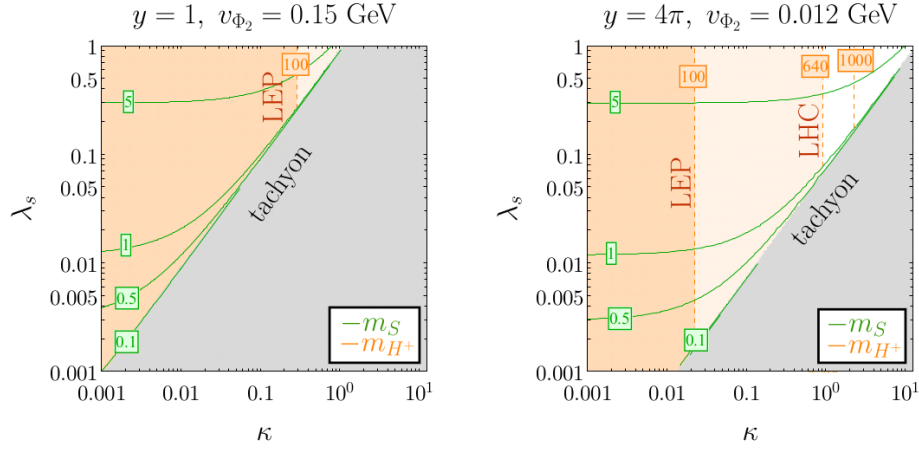


FIG. 3: Contours of s -like (green) and φ_2 -like (orange) scalar masses at two v_{Φ_2} choices (i.e. at two y muon Yukawa choices). The LHC limit on muonphilic H^+ scalars is shown, which pushes y to large values near the perturbative 4π value.

$\lambda_1 = 0.13$	$\lambda_2 = 0.13$	$v_s = 6.5$ GeV	
$\lambda_{1s} = 0.01$	$\lambda_{2s} = 0.01$	$\lambda_{12} = \lambda'_{12} = 0.1$	
Benchmark A	$\kappa = 0.4677$	$\lambda_s = 0.0329$	$y = 4\pi$
$(m_{H_1}, m_{H_2}, m_{H_3}) \approx (75 \text{ MeV}, 125 \text{ GeV}, 640 \text{ GeV})$			
Benchmark B	$\kappa = 2.308$	$\lambda_s = 0.1615$	$y = 4\pi$
$(m_{H_1}, m_{H_2}, m_{H_3}) \approx (80 \text{ MeV}, 125 \text{ GeV}, 1 \text{ TeV})$			

TABLE II: Scalar sector benchmarks. Parameters in the top cell are shared by both benchmarks.

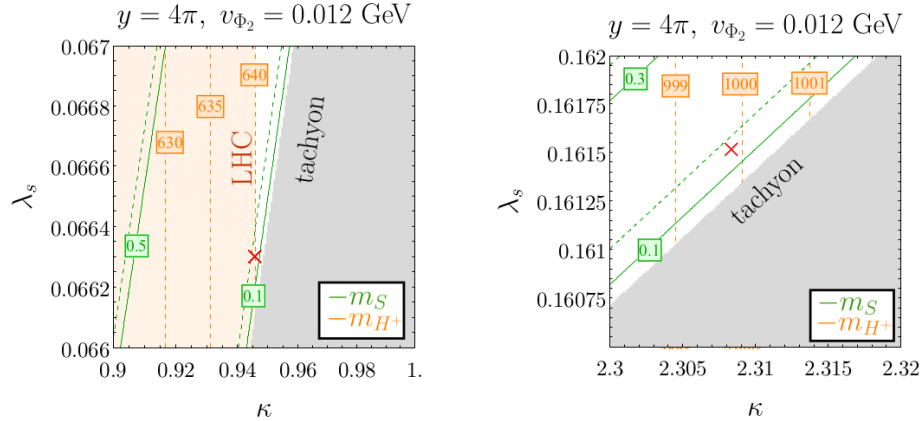


FIG. 4: Zooms of Fig. 3 right panel, one around the LHC limit on H^+ scalars (left) and the other around the $m_{H^+} = 1$ TeV mass contour. Red crosses mark the benchmarks in Table II.

We follow the mass ordering $m_{H_1} \leq m_{H_2} \leq m_{H_3}$, hence H_1 is a sub-GeV s -like light state, H_2 the SM-like Higgs, and H_3 is a heavier scalar (with the physical states mostly unmixed).

Having established the scalar mass spectrum one can also determine the size of the scalar-fermion couplings, such as, the scalar-muon and -quark couplings which are needed to compute the contribution of the scalars to the charge

radius Δr_p^2 . From Eq.(3), the scalar-muon couplings are given by

$$C_S^\mu[H_k] = -\frac{y}{\sqrt{2}}(\mathcal{O}_R)_{k3} \quad \text{with } k = 1, 2, 3, \quad (14)$$

where \mathcal{O}_R is the CP-even mixing matrix and is formally determined from Appendix A. Meanwhile, the scalar couplings to the proton are given by

$$C_S^p[H_k] = -\frac{y_q}{\sqrt{2}}(\mathcal{O}_R)_{k3} \quad \text{with } k = 1, 2, 3, \quad (15)$$

where y_q is the quark Yukawa. Using Eqs. (14) and (15), one can write one coupling in terms of the other as $C_S^q = (y_q/y) C_S^\mu \sim (m_u/m_\mu) C_S^\mu \approx 2 \times 10^{-2} C_S^\mu$. Numerically, at the benchmarks

$$(C_S^\mu[H_1], C_S^\mu[H_2], C_S^\mu[H_3]) \approx (-0.03, -4.8 \times 10^{-4}, -8.9), \quad C_P^\mu[A] \approx \tilde{C}_{S,P}^\mu[H^+] \approx C_S^\mu[H_3] \quad \text{in both } \mathbf{A} \text{ and } \mathbf{B} \quad (16)$$

The value of these couplings stays almost identical in either benchmark, since $y = 4\pi$ in both.

Plugging the resulting couplings and scalar masses into $\Delta E^{(S)}$, as in Eq. (6), one gets that the Higgs-like H_2 and H_3 provide a negligible contribution to Δr_p^2 . The sub-GeV scalar H_1 adds to the required energy shift at the level of 10%, representing a subleading contribution to the charge radius. This makes plausible to stick to the limit in which the Δr_p^2 deviation is addressed by Z' alone⁷.

B. The muon anomalous magnetic moment

As we have seen, our model is characterized by its mounphilic interactions, which give additional corrections to the muon anomalous magnetic moment, commonly parametrized as $\Delta a_\mu \equiv (g-2)_\mu/2$. Therefore, in what follows we show the allowed parameter space where our model simultaneously satisfies Δr_p^2 , the limits on the new scalars, and the constraints coming from latest $(g-2)_\mu$ results.

In light of the latest $(g-2)_\mu$ Fermilab measurement [4, 19], we interpret these results either as a bound on BSM states under the assumption that the SM deviation eventually fades away or as a hint of new physics. This is done by subtracting the $(g-2)_\mu$ measurement to two theory predictions, namely

$$\Delta a_\mu^{\text{latt}}/10^{-11} = 109 \pm 71, \quad (17)$$

$$\Delta a_\mu^{\text{SM,th}}/10^{-11} = 251 \pm 59. \quad (18)$$

Δa^{latt} is the current Fermilab+BNL average after subtracting the latest QCD theoretical prediction by lattice including vacuum hadron polarization [20]. A summary of more lattice results by other groups is discussed in Refs. [27, 28]. On the other hand, $\Delta a_\mu^{\text{SM,th}}$ is the current Fermilab+BNL average after subtracting the theoretical SM contribution [29].

In this scenario, Δa_μ receives contributions from all physical scalars and the new gauge boson, all of them are listed in Appendix B. Since the Z' couples exclusively to RH fermions,

$$C_V[Z'] = C_A[Z'] = -g'/2, \quad (19)$$

⁷ In contrast to our model, there exist scenarios that tackle r_p and the muon $(g-2)$ without a UV completion. See for instance Ref. [26] where a light electrophobic scalar fits r_p and the muon $(g-2)$ while satisfying related bounds due to its coupling to neutrons.

the contribution to $(g-2)_\mu$ is negative, given that the axial piece of Δa_μ is approximately 10 times larger than the vectorial one at equal couplings [30]. Fig. 5 shows $\Delta a_\mu^{(Z')}$ for different Z' masses and gauge couplings, displayed as solid blue contours in the $(g', m_{Z'})$ -plane. According to the lattice bound (solid red) in Eq. (17), $\Delta a_\mu^{(Z')} < 0$ is not excluded as long as its magnitude lies within its 2σ range, this would correspond to Δa_μ contours outside the red shaded region. However, notice that values allowed from the lattice constraint are incompatible with Δr_p^2 (solid black line). In other words, the safe region from the lattice constraint has smaller r_p than the required one to fit the charge radius discrepancy, as noticed in Refs. [15, 31].

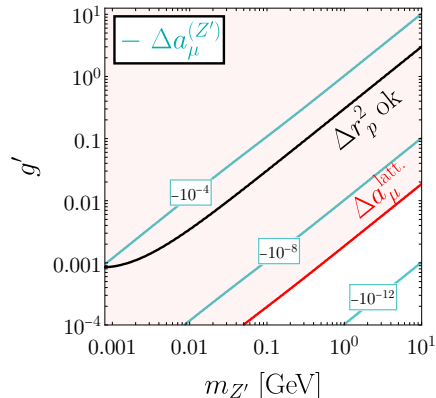


FIG. 5: $(g-2)_\mu$ contribution by a Z' coupled to RH fermions (cyan contours). The Δr_p^2 fitting curve is depicted in dashed black. The $(g-2)_\mu$ lattice bound exclusion from Eq. (17) is shaded red.

For the scalar contributions to Δa_μ one needs to extract their couplings to muons. The $H_{1,2,3}$ couplings are already listed in Eq. (14) and those of the physical pseudoscalar and the charged scalar are

$$C_P^\mu[A] = -\frac{y}{\sqrt{2}}(\mathcal{O}_I)_{33}, \quad \tilde{C}_{S,P}^\mu[H^+] = -\frac{1}{2}(-y \pm y_\nu)(\mathcal{O}_\pm)_{22}, \quad (20)$$

expressed in terms of the corresponding mixing matrices given in Appendix A. Since $y_\nu \sim m_\nu/v_{\Phi_2} \sim 10^{-8} \ll y$, the couplings $\tilde{C}_S^\mu[H^+]$ and $\tilde{C}_P^\mu[H^+]$ are practically the same which leads to a negligible contribution from the charged scalar to Δa_μ .

As we have seen, the parameter κ controls the masses of the heavy scalars and tends to be of order $\mathcal{O}(1)$, look at Fig. 3 for reference. This leads to a high degree of degeneracy of the φ_2 -like scalars. Then, the contributions to $(g-2)_\mu$ by near-degenerate CP-even and CP-odd scalars partially cancel among each other, for comparable couplings. This is similar to what occurs with the contribution from the charged scalar [30]. As a result, the only sizable scalar contribution to the anomalous magnetic moment of the muon comes from the s -like state H_1 with sub-GeV mass. We then look for regions of the parameter space where its contribution to $(g-2)_\mu$ together with that of the Z' satisfies the experimental constraints as well as explain the charge radius.

The left panel of Fig. 6 plots Δa_μ by the Z' alone (in blue) as a function of its mass, where at each $m_{Z'}$ the g' coupling shown in the top axis fits Δr_p^2 according to Fig. 2. Even though g' is varied, the required v_s for the corresponding $m_{Z'}$ in the bottom axis stays constant at the benchmark value as long as $m_{Z'}$ is above a few MeV. From the graph it is clear that $\Delta a_\mu^{(Z')}$ alone is too large and negative to hit either the $(g-2)_\mu$ lattice bound on new physics or the 2σ band of the tentative signal. Here is where the light s -like scalar remedies this situation: the black curves in the same panel indicate the combined Δa_μ by Z' and s , evaluated at the scalar-muon couplings (16). One sees that for tens of MeV it is possible for the black curves to hit the region relevant for $(g-2)_\mu$ bounds. The right

panel of Fig. 6 zooms in into the lattice bound (red dashed) and signal hint (green band) ballpark. Therefore, the model is capable of simultaneously fit Δr_p^2 and be compatible with $(g-2)_\mu$ measurements, while generating the muon mass and evading current collider constraints on heavy scalars.

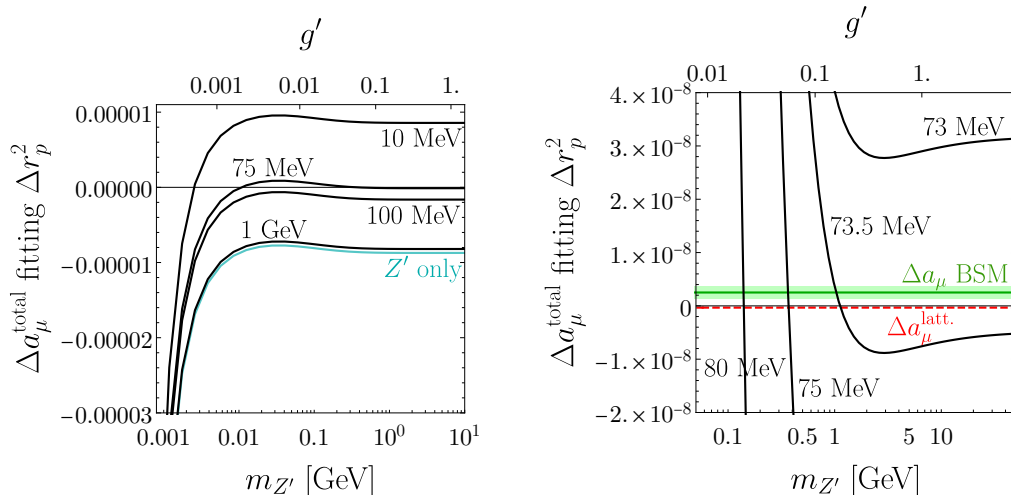


FIG. 6: **Left:** Z' -only (blue curve) and joint $Z' + s$ contribution to $(g-2)_\mu$ (black curves). The vertical g' ticks indicate corresponding gauge coupling values fitting Δr_p^2 at each $m_{Z'}$. **Right:** Zoomed region for the $(g-2)_\mu$ lattice bound (dashed red) and 2σ band of the new physics hint (green).

C. Further restrictions on Z'

Before concluding, we briefly mention constraints that may apply to our specific kind of Z' . First, our Z' expects to face looser constraints compared to other types of Z' s that couple to electrons at tree-level⁸. For instance, this Z' automatically avoids the stringent limits from rare pion decays $\pi^0 \rightarrow \gamma Z' \rightarrow \gamma(e^+e^-)$ and $\nu - e$ scattering.

μ -flavored Z' s are however subject to a variety of limits [32]. For $m_{Z'}$ exceeding the $\mu^+\mu^-$ threshold, there are CMS and BaBar searches on $Z'Z' \rightarrow 4\mu$ as well as $B^+ \rightarrow K^+Z' \rightarrow K^+(\mu^+\mu^-)$ in LHCb. Below the $\mu^+\mu^-$ threshold there are $\pi^0 \rightarrow \gamma Z' \rightarrow \gamma(\nu\nu)$ decay constraints. Due to possible kinetic mixing and its modification to $m_{Z'}$, there are also bounds from atomic parity violation and the electroweak T -parameter.

More importantly, there are current stringent constraints on the $(m_{Z'}, \varepsilon)$ plane, where $\varepsilon = eg'/(16\pi^2)$ is the kinetic mixing parameter. See for instance the limits by the NA64 and other collaborations in Ref. [33]. A simple analysis shows that the model is consistent in a wide region of the allowed parameter space. In addition, there are neutrino-related bounds from non-standard induced ν -interactions, or coherent elastic neutrino nucleus scattering. At masses near 10 MeV there are also ΔN_{eff} constraints on dark radiation degrees of freedom.

It is worth mentioning that a variety of nuclear experiments impose bounds on the ratio C_V^n/C_V^p of neutron- Z' to proton- Z' coupling, where $C_V^n = C_V^u + 2C_V^d$ and $C_V^p = 2C_V^u + C_V^d$. For example, measurements on another muon-nucleus bound state, the Muonic Deuterium (μD), put important exclusion limits on this ratio. From Ref. [26], one can see that results on μD allow the window $-1 \lesssim C_V^n/C_V^p \lesssim 0$ for $m_{Z'} < 100$ MeV. In our setup, see Sec. II, given that the $U(1)_R$ charge assignments for u and d are fully determined by $q_\nu = 1$, the ratio of neutron- and proton- Z'

⁸ Coupling to e^+e^- here is induced by kinetic mixing only.

couplings satisfies $C_V^n/C_V^p = -1$ for $m_{Z'}$ in the 10-100 MeV range. This small tension with the μ D constraint can be easily diluted if the u and d are placed in distinct anomaly-free sets. That is, for instance, taking another anomaly free solution $\{u_R, b_R, \mu_R, \nu_R\}$ with $U(1)_R$ charge parametrized by q_ν and $\{c_R, d_R, \tau_R, \nu'_R\}$ parametrized by $q'_\nu \neq q_\nu$, then $C_V^n/C_V^p = (2q_\nu - q'_\nu)/(-2q'_\nu + q_\nu)$ can be varied and brought to safety from the μ D limits while leaving our general conclusions for Δr_p^2 and $(g-2)_\mu$ unaffected⁹. A detailed analysis of the multitude of bounds on Z' is left for an upcoming work [34]. The general Z' constraints mentioned above must be implemented by taking into account 1) that Z' is coupled to RH fermions only, and 2) that we have at our disposal some freedom in the quark sector to lock the RH quark rotations as diagonal matrices, and to turn off some u and d Yukawas to avoid dangerous H^+ -mediated meson processes.

V. CONCLUSIONS

Every few years during the last decade muons have receive renewed attention from the community. This has been a consequence of the various experimental results that have hinted at new physics, among which two good examples are the B -meson decay anomalies and the muon $(g-2)$ measurement. Other less known instances, such as the proton charge radius, are also exciting venues for searches of discoveries beyond the Standard Model.

Before the seemingly surviving discrepancy in the proton charge radius succumbs to the improvement in precision techniques or better yet, a discovery is made, models accommodating it can be implemented and tested. This work proposes a SM extension based on a $U(1)_R$ gauge boson with exclusive coupling to right-handed muons, up and down quarks at tree-level, that addresses the Δr_p discrepancy for sub-GeV Z' . Spontaneous breaking of the $U(1)_R$, the generation of the μ, u , and d masses, and agreement with the recent $(g-2)$ measurements demand extra scalar degrees of freedom. The new scalar states can be brought to consistency with LHC limits albeit in a tight region of the parameter space, with a light singlet-like scalar at the tens of MeV, and doublet-like, near-degenerate neutral, charged and pseudoscalar states no lighter than ~ 640 GeV. Further constraints arise for the gauge boson that deserve a study on its own, focusing on the preferential coupling of the Z' to right-handed chiral fermions.

ACKNOWLEDGMENTS

A.A. acknowledges support from SNI-CONACYT. The work of C.B. has been supported by ANID under the FONDECYT grant “Nu Physics” No. 11201240. C.A. thanks the Facultad de Ciencias of the Universidad de Colima for its hospitality.

Appendix A: Mass mixing and spectra

1. Scalar sector

After acquiring vacuum expectation values (vevs) the fields are shifted as follows,

$$\varphi_i^0 = \frac{1}{\sqrt{2}} (v_{\Phi_i} + \varphi_{R_1} + i\varphi_{I_1}), \quad \text{and} \quad s = \frac{1}{\sqrt{2}} (v_s + s_R + is_I), \quad (\text{A1})$$

⁹ Certainly one more doublet Φ_3 is required to provide masses to c, d, τ , which simply duplicates the spectrum of heavy Higgses H^0, A^0, H^\pm .

so the extremum conditions are

$$\begin{aligned}\mu_1^2 &= \frac{1}{2} \left(2\lambda_1 v_{\Phi_1}^2 + \lambda_{1s} v_s^2 + (\lambda_{12} + \lambda'_{12}) v_{\Phi_2}^2 - \frac{\kappa v_s^2 v_{\Phi_2}}{v_{\Phi_1}} \right), \\ \mu_2^2 &= \frac{1}{2} \left((\lambda_{12} + \lambda'_{12}) v_{\Phi_1}^2 + \lambda_{2s} v_s^2 + 2\lambda_2 v_{\Phi_2}^2 - \frac{\kappa v_{\Phi_1} v_s^2}{v_{\Phi_2}} \right), \\ \mu_s^2 &= \frac{1}{2} (\lambda_{1s} v_{\Phi_1}^2 + \lambda_{2s} v_{\Phi_2}^2 + 2\lambda_s v_s^2 - 2\kappa v_{\Phi_1} v_{\Phi_2}).\end{aligned}\quad (\text{A2})$$

Upon minimization, the scalar mass matrices read

$$M_R^2 = \begin{pmatrix} 2\lambda_1 v_{\Phi_1}^2 + \frac{\kappa v_s^2 v_{\Phi_2}}{2v_{\Phi_1}} & (\lambda_{1s} v_{\Phi_1} - \kappa v_{\Phi_2}) v_s & (\lambda_{12} + \lambda'_{12}) v_{\Phi_1} v_{\Phi_2} - \frac{\kappa v_s^2}{2} \\ (\lambda_{1s} v_{\Phi_1} - \kappa v_{\Phi_2}) v_s & 2\lambda_s v_s^2 & (\lambda_{2s} v_{\Phi_2} - \kappa v_{\Phi_1}) v_s \\ (\lambda_{12} + \lambda'_{12}) v_{\Phi_1} v_{\Phi_2} - \frac{\kappa v_s^2}{2} & (\lambda_{2s} v_{\Phi_2} - \kappa v_{\Phi_1}) v_s & 2\lambda_2 v_{\Phi_2}^2 + \frac{\kappa v_{\Phi_1} v_s^2}{2v_{\Phi_2}} \end{pmatrix} \quad (\text{A3})$$

and

$$M_I^2 = \kappa \begin{pmatrix} \frac{v_s^2 v_{\Phi_2}}{2v_{\Phi_1}} & -v_s v_{\Phi_2} & -\frac{v_s^2}{2} \\ -v_s v_{\Phi_2} & 2v_{\Phi_1} v_{\Phi_2} & v_{\Phi_1} v_s \\ -\frac{v_s^2}{2} & v_{\Phi_1} v_s & \frac{v_{\Phi_1} v_s^2}{2v_{\Phi_2}} \end{pmatrix}. \quad (\text{A4})$$

Define the rotation matrices \mathcal{O}_R and \mathcal{O}_I according to $\text{diag}(m_{H_1}^2, m_{H_2}^2, m_{H_3}^2) = \mathcal{O}_R M_R^2 \mathcal{O}_R^T$ and $\text{diag}(0, 0, m_A^2) = \mathcal{O}_I M_I^2 \mathcal{O}_I^T$, then

$$m_A^2 = \frac{\kappa (v_{\Phi_1}^2 (v_s^2 + 4v_{\Phi_2}^2) + v_s^2 v_{\Phi_2}^2)}{2v_{\Phi_1} v_{\Phi_2}}, \quad \mathcal{O}_I = \begin{pmatrix} \alpha v_{\Phi_1} & 0 & \alpha v_{\Phi_2} \\ -2\alpha\beta v_{\Phi_1} v_{\Phi_2}^2 & -\frac{\beta}{\alpha} v_s & 2\alpha\beta v_{\Phi_1}^2 v_{\Phi_2} \\ -\beta v_s v_{\Phi_2} & 2\beta v_{\Phi_1} v_{\Phi_2} & \beta v_{\Phi_1} v_s \end{pmatrix} \quad (\text{A5})$$

where

$$\alpha = \frac{1}{\sqrt{v_{\Phi_1}^2 + v_{\Phi_2}^2}}, \quad \beta = \frac{1}{\sqrt{4v_{\Phi_1}^2 v_{\Phi_2}^2 + v_{\Phi_1}^2 v_s^2 + v_{\Phi_2}^2 v_s^2}}. \quad (\text{A6})$$

Unless κ is tiny, neither the CP-even (squared) masses $m_{H_k}^2$ nor \mathcal{O}_R have a simple analytical form, they are numerically evaluated instead. Turning now to the charged sector we have, in the basis $(\varphi_1^+, \varphi_2^+)$, the following mass squared matrix

$$M_{\pm}^2 = \frac{1}{2} \begin{pmatrix} \left(-\lambda'_{12} v_{\Phi_2} + \frac{\kappa v_s^2}{v_{\Phi_1}} \right) v_{\Phi_2} & \lambda'_{12} v_{\Phi_1} v_{\Phi_2} - \kappa v_s^2 \\ \lambda'_{12} v_{\Phi_1} v_{\Phi_2} - \kappa v_s^2 & \left(-\lambda'_{12} v_{\Phi_1} + \frac{\kappa v_s^2}{v_{\Phi_2}} \right) v_{\Phi_1} \end{pmatrix}, \quad (\text{A7})$$

whose eigenstates are the longitudinal W^{\pm} boson and the physical H^{\pm} . The (squared) masses and rotation matrix satisfying $\text{diag}(0, m_{H_{\pm}}^2) = \mathcal{O}_{\pm} M_{\pm}^2 \mathcal{O}_{\pm}^T$ are

$$m_{H^{\pm}}^2 = \frac{1}{2} (v_{\Phi_1}^2 + v_{\Phi_2}^2) \left(-\lambda'_{12} + \frac{\kappa v_s^2}{v_{\Phi_1} v_{\Phi_2}} \right), \quad \mathcal{O}_{\pm} = \begin{pmatrix} \alpha v_{\Phi_1} & \alpha v_{\Phi_2} \\ -\alpha v_{\Phi_2} & \alpha v_{\Phi_1} \end{pmatrix}. \quad (\text{A8})$$

2. Charged fermion sector

From Eq. (3), the textures of the charged fermion mass matrices are

$$M_{\ell} = \begin{pmatrix} y_{1e} v_{\Phi_1} & y_{1\mu} v_{\Phi_2} & y_{1\tau} v_{\Phi_1} \\ y_{2e} v_{\Phi_1} & y_{2\mu} v_{\Phi_2} & y_{2\tau} v_{\Phi_1} \\ y_{3e} v_{\Phi_1} & y_{3\mu} v_{\Phi_2} & y_{3\tau} v_{\Phi_1} \end{pmatrix}, \quad (\text{A9})$$

$$M_d = \begin{pmatrix} y_{1d}v_{\Phi_2} & y_{1s}v_{\Phi_1} & y_{1b}v_{\Phi_1} \\ y_{2d}v_{\Phi_2} & y_{2s}v_{\Phi_1} & y_{2b}v_{\Phi_1} \\ y_{3d}v_{\Phi_2} & y_{3s}v_{\Phi_1} & y_{3b}v_{\Phi_1} \end{pmatrix}, \quad (\text{A10})$$

$$M_u = \begin{pmatrix} y_{1u}v_{\Phi_2} & y_{1c}v_{\Phi_1} & y_{1t}v_{\Phi_1} \\ y_{2u}v_{\Phi_2} & y_{2c}v_{\Phi_1} & y_{2t}v_{\Phi_1} \\ y_{3u}v_{\Phi_2} & y_{3c}v_{\Phi_1} & y_{3t}v_{\Phi_1} \end{pmatrix}. \quad (\text{A11})$$

Given the number of Yukawas in the up and down quark mass matrices, the Cabbibo-Kobayashi-Maskawa mixing matrix can be straightforwardly fitted.

Appendix B: Δa_μ contributions

The notation and normalization for the muon couplings in Secs. III and IV is adopted from Ref. [35], with S , P denoting true scalar and pseudoscalar, V and A polar and axial vector, and \tilde{S} , \tilde{P} referring to charged scalar couplings

$$\begin{aligned} \mathcal{L} \supset & C_S^{ij} \phi^0 \bar{\ell}_i \ell_j + C_P^{ij} \phi^0 \bar{\ell}_i \gamma_5 \ell_j \\ & + \left(\tilde{C}_S^{ij} \phi^+ \bar{\nu}_i \ell_j + \tilde{C}_P^{ij} \phi^+ \bar{\nu}_i \gamma_5 \ell_j + \text{H.c.} \right) \\ & + \left(C_V^{ij} Z'_\mu \bar{\ell}_i \gamma^\mu \ell_j + C_A^{ij} Z'_\mu \bar{\ell}_i \gamma^\mu \gamma^5 \ell_j + \text{H.c.} \right). \end{aligned} \quad (\text{B1})$$

With vanishing charged lepton mixing, for $i = j = \mu$

$$\Delta a_\mu^{(Z')} = \frac{1}{8\pi^2} \frac{m_\mu^2}{m_{Z'}^2} \int_0^1 dx \frac{|C_V[Z']|^2 P_V(x) + |C_A[Z']|^2 P_A(x)}{(1-x)(1-m_\mu^2/m_{Z'}^2) + x(m_\mu^2/m_{Z'}^2)} \quad (\text{B2})$$

where

$$P_{V,A}(x) \equiv 2x(1-x)(x-2 \pm 2) + (m_\mu^2/m_{Z'}^2)x^2(1 \mp 1)^2(1-x \pm 1). \quad (\text{B3})$$

For the CP -even scalars H_k ,

$$\Delta a_\mu^{(H_k)} = \frac{1}{8\pi^2} \frac{m_\mu^2}{m_{H_k}^2} \int_0^1 dx \frac{|C_S^\mu[H_k]|^2 P_S(x)}{(1-x)(1-m_\mu^2/m_{H_k}^2) + x(m_\mu^2/m_{H_k}^2)} \quad (\text{B4})$$

with

$$P_S(x) \equiv x^2(2-x). \quad (\text{B5})$$

The analog pseudoscalar and charged scalar contributions are listed below,

$$\Delta a_\mu^{(A)} = \frac{1}{8\pi^2} \frac{m_\mu^2}{m_A^2} \int_0^1 dx \frac{|C_P^\mu[A]|^2 P_P(x)}{(1-x)(1-m_\mu^2/m_A^2) + x(m_\mu^2/m_A^2)} \quad (\text{B6})$$

with

$$P_P(x) \equiv -x, \quad (\text{B7})$$

and

$$\Delta a_\mu^{(H^+)} = \frac{1}{8\pi^2} \frac{m_\mu^2}{m_{H^+}^2} \int_0^1 dx \frac{|\tilde{C}_S^\mu[H^+]|^2 P_{\tilde{S}}(x) + |\tilde{C}_P^\mu[H^+]|^2 P_{\tilde{P}}(x)}{(1-x)(1-m_\mu^2/m_{H^+}^2) + x(m_\mu^2/m_{H^+}^2)} \quad (\text{B8})$$

where

$$P_{\tilde{S},\tilde{P}}(x) \equiv x(1-x)(x \pm 1) . \quad (\text{B9})$$

-
- [1] C. Bonilla, T. Modak, R. Srivastava, and J. W. F. Valle, “ $U(1)_{B_3-3L_\mu}$ gauge symmetry as a simple description of $b \rightarrow s$ anomalies,” *Phys. Rev. D* **98** no. 9, (2018) 095002, [arXiv:1705.00915 \[hep-ph\]](#).
- [2] **LHCb** Collaboration, R. Aaij *et al.*, “Test of lepton universality in beauty-quark decays,” [arXiv:2103.11769 \[hep-ex\]](#).
- [3] W. Altmannshofer and P. Stangl, “New Physics in Rare B Decays after Moriond 2021,” [arXiv:2103.13370 \[hep-ph\]](#).
- [4] **Muon g-2** Collaboration, B. Abi *et al.*, “Measurement of the Positive Muon Anomalous Magnetic Moment to 0.46 ppm,” *Phys. Rev. Lett.* **126** no. 14, (2021) 141801, [arXiv:2104.03281 \[hep-ex\]](#).
- [5] R. Pohl *et al.*, “The size of the proton,” *Nature* **466** (2010) 213–216.
- [6] A. Antognini, F. Nez, and Schuhmann, “Proton structure from the measurement of 2s-2p transition frequencies of muonic hydrogen,” *Science* **339** no. 6118, (2013) 417–420.
- [7] P. J. Mohr, D. B. Newell, and B. N. Taylor, “CODATA Recommended Values of the Fundamental Physical Constants: 2014,” *Rev. Mod. Phys.* **88** no. 3, (2016) 035009, [arXiv:1507.07956 \[physics.atom-ph\]](#).
- [8] E. Tiesinga, P. J. Mohr, D. B. Newell, and B. N. Taylor, “Codata recommended values of the fundamental physical constants: 2018,” *Rev. Mod. Phys.* **93** (Jun, 2021) 025010. <https://link.aps.org/doi/10.1103/RevModPhys.93.025010>.
- [9] N. Bezginov, T. Valdez, M. Horbatsch, A. Marsman, A. C. Vutha, and E. A. Hessels, “A measurement of the atomic hydrogen lamb shift and the proton charge radius,” *Science* **365** no. 6457, (2019) 1007–1012, <https://science.sciencemag.org/content/365/6457/1007.full.pdf>, <https://science.sciencemag.org/content/365/6457/1007>.
- [10] H. Fleurbaey, S. Galtier, S. Thomas, M. Bonnaud, L. Julien, F. m. c. Biraben, F. m. c. Nez, M. Abgrall, and J. Guéna, “New measurement of the $1s - 3s$ transition frequency of hydrogen: Contribution to the proton charge radius puzzle,” *Phys. Rev. Lett.* **120** (May, 2018) 183001. <https://link.aps.org/doi/10.1103/PhysRevLett.120.183001>.
- [11] M. Mihovilović *et al.*, “The proton charge radius extracted from the initial-state radiation experiment at MAMI,” *Eur. Phys. J. A* **57** no. 3, (2021) 107, [arXiv:1905.11182 \[nucl-ex\]](#).
- [12] C. E. Carlson, “The Proton Radius Puzzle,” *Prog. Part. Nucl. Phys.* **82** (2015) 59–77, [arXiv:1502.05314 \[hep-ph\]](#).
- [13] H. Gao and M. Vanderhaeghen, “The proton charge radius,” [arXiv:2105.00571 \[hep-ph\]](#).
- [14] A. Grinin, A. Matveev, D. C. Yost, L. Maisenbacher, V. Wirthl, R. Pohl, T. W. Hänsch, and T. Udem, “Two-photon frequency comb spectroscopy of atomic hydrogen,” *Science* **370** no. 6520, (2020) 1061–1066, <https://science.sciencemag.org/content/370/6520/1061.full.pdf>, <https://science.sciencemag.org/content/370/6520/1061>.
- [15] C. E. Carlson and B. C. Rislow, “New Physics and the Proton Radius Problem,” *Phys. Rev. D* **86** (2012) 035013, [arXiv:1206.3587 \[hep-ph\]](#).
- [16] B. Batell, D. McKeen, and M. Pospelov, “New Parity-Violating Muonic Forces and the Proton Charge Radius,” *Phys. Rev. Lett.* **107** (2011) 011803, [arXiv:1103.0721 \[hep-ph\]](#).
- [17] M. Perelstein and Y. C. San, “Dark Matter as a Solution to Muonic Puzzles,” *Phys. Rev. D* **103** no. 3, (2021) 035032, [arXiv:2009.09867 \[hep-ph\]](#).
- [18] B. Zhu and X. Liu, “Probing the flavor-specific scalar mediator for the muon ($g - 2$) deviation, the proton radius puzzle and the light dark matter production,” [arXiv:2104.03238 \[hep-ph\]](#).
- [19] **Muon g-2** Collaboration, T. Albahri *et al.*, “Magnetic-field measurement and analysis for the Muon $g - 2$ Experiment at Fermilab,” *Phys. Rev. A* **103** no. 4, (2021) 042208, [arXiv:2104.03201 \[hep-ex\]](#).

- [20] S. Borsanyi *et al.*, “Leading hadronic contribution to the muon $g-2$ magnetic moment from lattice QCD,” [arXiv:2002.12347 \[hep-lat\]](#).
- [21] P. Fayet, “Extra $u(1)$ ’s and new forces,” *Nuclear Physics B* **347** no. 3, (1990) 743–768. <https://www.sciencedirect.com/science/article/pii/055032139090381M>.
- [22] P. Fayet, “The light U boson as the mediator of a new force, coupled to a combination of Q, B, L and dark matter,” *Eur. Phys. J. C* **77** no. 1, (2017) 53, [arXiv:1611.05357 \[hep-ph\]](#).
- [23] C. Bonilla and J. W. F. Valle, “Naturally light neutrinos in *Diracon* model,” *Phys. Lett. B* **762** (2016) 162–165, [arXiv:1605.08362 \[hep-ph\]](#).
- [24] M. Lindner, F. S. Queiroz, W. Rodejohann, and X.-J. Xu, “Neutrino-electron scattering: general constraints on Z' and dark photon models,” *JHEP* **05** (2018) 098, [arXiv:1803.00060 \[hep-ph\]](#).
- [25] T. Abe, R. Sato, and K. Yagyu, “Muon specific two-Higgs-doublet model,” *JHEP* **07** (2017) 012, [arXiv:1705.01469 \[hep-ph\]](#).
- [26] Y.-S. Liu, D. McKeen, and G. A. Miller, “Electrophobic Scalar Boson and Muonic Puzzles,” *Phys. Rev. Lett.* **117** no. 10, (2016) 101801, [arXiv:1605.04612 \[hep-ph\]](#).
- [27] A. Gérardin, “The anomalous magnetic moment of the muon: status of Lattice QCD calculations,” *Eur. Phys. J. A* **57** no. 4, (2021) 116, [arXiv:2012.03931 \[hep-lat\]](#).
- [28] M. Davier, A. Hoecker, B. Malaescu, and Z. Zhang, “A new evaluation of the hadronic vacuum polarisation contributions to the muon anomalous magnetic moment and to $\alpha(\mathbf{m}_Z^2)$,” *Eur. Phys. J. C* **80** no. 3, (2020) 241, [arXiv:1908.00921 \[hep-ph\]](#). [Erratum: *Eur.Phys.J.C* 80, 410 (2020)].
- [29] T. Aoyama *et al.*, “The anomalous magnetic moment of the muon in the Standard Model,” *Phys. Rept.* **887** (2020) 1–166, [arXiv:2006.04822 \[hep-ph\]](#).
- [30] F. Jegerlehner and A. Nyffeler, “The Muon $g-2$,” *Phys. Rept.* **477** (2009) 1–110, [arXiv:0902.3360 \[hep-ph\]](#).
- [31] D. V. Kirpichnikov, V. E. Lyubovitskij, and A. S. Zhevlakov, “Implication of hidden sub-GeV bosons for the $(g-2)_\mu$, ^8Be - ^4He anomaly, proton charge radius, EDM of fermions, and dark axion portal,” *Phys. Rev. D* **102** no. 9, (2020) 095024, [arXiv:2002.07496 \[hep-ph\]](#).
- [32] M. Bauer, P. Foldenauer, and M. Mosny, “Flavor structure of anomaly-free hidden photon models,” *Phys. Rev. D* **103** no. 7, (2021) 075024, [arXiv:2011.12973 \[hep-ph\]](#).
- [33] D. Banerjee *et al.*, “Dark matter search in missing energy events with NA64,” *Phys. Rev. Lett.* **123** no. 12, (2019) 121801, [arXiv:1906.00176 \[hep-ex\]](#).
- [34] C. Alvarado, A. Aranda, and C. Bonilla, “In progress,” [arXiv:2112.XXXXX \[hep-ph\]](#).
- [35] M. Lindner, M. Platscher, and F. S. Queiroz, “A Call for New Physics : The Muon Anomalous Magnetic Moment and Lepton Flavor Violation,” *Phys. Rept.* **731** (2018) 1–82, [arXiv:1610.06587 \[hep-ph\]](#).